

# Unsupervised optimal deep transfer learning for classification under general conditional shift

Junjun Lang<sup>1</sup> and Yukun Liu<sup>\*1</sup>

<sup>1</sup> KLATASDS-MOE, School of Statistics, East China Normal University, Shanghai 200062, China

## Abstract

Classifiers trained solely on labeled source data may yield misleading results when applied to unlabeled target data drawn from a different distribution. Transfer learning can rectify this by transferring knowledge from source to target data, but its effectiveness frequently relies on stringent assumptions, such as label shift. In this paper, we introduce a novel General Conditional Shift (GCS) assumption, which encompasses label shift as a special scenario. Under GCS, we demonstrate that both the target distribution and the shift function are identifiable. To estimate the conditional probabilities  $\eta_P$  for source data, we propose leveraging deep neural networks (DNNs). Subsequent to transferring the DNN estimator, we estimate the target label distribution  $\pi_Q$  utilizing a pseudo-maximum likelihood approach. Ultimately, by incorporating these estimates and circumventing the need to estimate the shift function, we construct our proposed Bayes classifier. We establish concentration bounds for our estimators of both  $\eta_P$  and  $\pi_Q$  in terms of the intrinsic dimension of  $\eta_P$ . Notably, our DNN-based classifier achieves the optimal minimax rate, up to a logarithmic factor. A key advantage of our method is its capacity to effectively combat the curse of dimensionality when  $\eta_P$  exhibits a low-dimensional structure. Numerical simulations, along with an analysis of an Alzheimer’s disease dataset, underscore its exceptional performance.

**Keywords:** Transfer Learning; Deep Neural Network; General Conditional Shift; Classification; Minimax Optimality

---

\*Corresponding author: ykliu@sfs.ecnu.edu.cn

# 1 Introduction

Classifiers trained using labelled source data are typically employed to classify unlabelled target data that follow the same distribution. When the target data distribution deviates from that of the source data, the classifiers may lead to biased or misleading conclusions. Transfer learning is capable of correcting such classifiers by integrating information from both the labelled source data and the unlabelled target data. Generally speaking, transfer learning, also known as domain adaptation, arises in situations where the availability of data from the target domain is limited, whereas a considerable amount of data exists in a related source domain, thereby enabling knowledge transfer from the latter to the former. It has attracted significant attention across a wide variety of applications, particularly in computer vision (Tzeng *et al.*, 2017), speech recognition (Huang *et al.*, 2013), and machine learning (Iman *et al.*, 2023). See Weiss *et al.* (2016) and Zhuang *et al.* (2020) for more information regarding transfer learning and its applications. This paper focuses on transfer learning within the framework of nonparametric classification and is committed to utilizing modern deep learning techniques to develop an efficient algorithm that adapts classifiers trained on the source to the target domain under a general distribution shift assumption.

## 1.1 Problem statement

Let  $X \in \mathcal{X} \subset \mathbb{R}^d$  for  $d \geq 1$  denote a vector of covariates or features and let  $Y \in \mathcal{Y} \subset \mathbb{R}$  represent a discrete outcome or label. Denote the joint distributions of  $(X, Y)$  from the source and target domains by  $P_{(X,Y)}$  and  $Q_{(X,Y)}$ , respectively. Suppose that we have labelled source data and unlabelled or unsupervised target data,

$$(X_1^P, Y_1^P), \dots, (X_{n_P}^P, Y_{n_P}^P) \stackrel{i.i.d}{\sim} P_{(X,Y)}, \quad X_1^Q, \dots, X_{n_Q}^Q \stackrel{i.i.d}{\sim} Q_X, \quad (1)$$

where  $Q_X$  is the distribution function or probability measure of  $X$  in the target domain. Because the labels of the target data are unavailable, it is challenging, if not impossible, to learn a classifier with theoretical guarantee for the target data based solely on the target data themselves. This goal can be achieved by transferring information from the source data to the target data. A typical example is medical diagnosis, where  $X$  usually represents the physical indicators of patients that are relatively easy to measure, while

$Y$  measures the quality of the patient’s condition after treatment, which is often costly or difficult to measure. To save costs, doctors may wish to infer whether patients can end treatment based on the data of previous patients combined with the easily measurable physical indicators of the current patients.

Transfer learning or domain adaptation is impossible without underlying assumptions (Ben-David *et al.*, 2010). Its validity hinges on the similarity between the distributions of source and target data. Within this framework, two prominent similarity assumptions are covariate shift (Kpotufe and Martinet, 2021; Sugiyama *et al.*, 2008) and label shift (Saerens *et al.*, 2002; Maity *et al.*, 2022). In the scenario of covariate shift, the conditional distributions of  $Y$  given  $X$  remain consistent between the source and target data. Consequently, classifiers trained using source data yield valid predictions when directly employed on target data. Let  $P_{X|Y}(x | y)$  and  $Q_{X|Y}(x | y)$  be the probability density or mass functions of  $X$  given  $Y = y$  in the source and target domains, respectively. Conversely, label shift posits that  $P_{X|Y}(x | y) = Q_{X|Y}(x | y)$  and the marginal distributions of  $Y$  may diverge between the source and target domains. Label shift typically arises when external factors alter the distribution of labels. For instance, in medical diagnosis, symptoms (features) are often indicative of diseases (labels), but the distribution of diseases itself may shift.

Despite its widespread popularity in the realm of transfer learning, the label shift assumption may be restrictive, prohibiting any alterations in the conditional distribution of  $X$  given  $Y$ . For instance, the advent of COVID-19 has demonstrated that, even when a patient’s disease is known, the distribution of their symptoms can change post-pandemic. To accommodate such variations, we propose relaxing the label shift assumption and adopting a more general distribution shift assumption:

**Assumption 1** (General Conditional Shift, GCS). *There exists a function class  $\mathcal{H}$  on  $\mathcal{X}$  containing the constant function 1 such that for a function  $h(\cdot) \in \mathcal{H}$ ,*

$$\frac{Q_{X|Y}(x | y)}{P_{X|Y}(x | y)} = h(x), \quad \forall x \in \mathcal{X}, y \in \mathcal{Y}. \quad (2)$$

The GCS assumption stipulates that the ratios of the conditional densities of  $X$  given  $Y = y$  in the target and source domains are equivalent to a common function  $h(x)$  for all values of  $y$ . When the function class  $\mathcal{H}$  comprises solely the element 1, this assumption simplifies to label shift. Furthermore, it can be perceived as a modification

of the conditional shift proposed by Liu *et al.* (2021) or the exponential tilting model presented by Maity *et al.* (2023).

## 1.2 Our contributions

In this paper, we develop a minimax optimal classifier for unsupervised target data under the GCS assumption by leveraging knowledge transferred from the source domain using deep neural networks (DNNs). Our contributions are outlined as follows:

1. We introduce a novel distribution shift assumption, namely the GCS model presented in (2), which encompasses the traditional label shift assumption as a special case. The GCS model not only provides greater flexibility compared to label shift but also enables the identification and consistent estimation for the classification function of target domain by utilizing information from both source and target data.
2. Under the GCS assumption, we incorporate DNNs into transfer learning for classification tasks based on labeled source data and unlabeled target data. In contrast, traditional non-parametric methods, such as kernel-based techniques (Maity *et al.*, 2022) or the K-NN method (Cai and Wei, 2021), have been utilized for this purpose in the existing literature. Given the DNN estimator of  $\boldsymbol{\eta}_P(x)$ , the classification function of source domain, we introduce a pseudo-maximum likelihood estimator  $\hat{\boldsymbol{\pi}}_Q$  for the marginal distribution or class proportion  $\boldsymbol{\pi}_Q$  of the label  $Y$  in the target domain. We establish concentration bounds for both the DNN estimator of  $\boldsymbol{\eta}_P(x)$  and  $\hat{\boldsymbol{\pi}}_Q$ . Subsequently, the proposed classifier, which serves as an estimator of the Bayes classifier for the target data, is constructed by integrating these two estimators. One of the most fascinating features of our method lies in its ingenious way of circumventing the necessity of estimating the unknown function  $h(\cdot)$  in the GCS model (2).
3. We assume that the regression or classification function of the source domain belongs to the *composite smoothness function class* (Schmidt-Hieber, 2020), and demonstrate that the convergence rate of our proposed classifier is contingent upon the intrinsic dimension of the ideal classification function. Our method is capable of mitigating the curse-of-dimensionality when the classification function

in the source domain exhibits a certain low-dimensional structure (Schmidt-Hieber, 2020; Zhong *et al.*, 2022). In contrast, existing works on transfer learning for classification (Maity *et al.*, 2022; Cai and Wei, 2021; Liu *et al.*, 2020) typically grapple with the curse-of-dimensionality issue, where the convergence rates of their classifiers can be extremely slow in the presence of high-dimensional covariates.

4. We derive the minimax optimal convergence rate for classifiers in the target domain in terms of excess risk in general multi-class settings. Our findings reveal that the proposed DNN-based classifier attains the optimal minimax rate, asymptotically up to a logarithmic factor. These results constitute novel contributions to the literature on unsupervised transfer learning for classification, particularly in scenarios involving labeled source data and unlabeled target data.

In summary, under the GCS model and within a multi-class setting, we have established theoretical guarantees for our DNN-based estimators concerning the classification function in the source domain and class proportions in the unlabeled target domain. Leveraging the strengths of deep transfer learning, we have developed an efficient classifier specifically designed for the target domain. This classifier has demonstrated its prowess in addressing the curse of dimensionality, achieving minimax optimality, and exhibiting remarkable efficacy in a real-world application.

### 1.3 Related works

The GCS assumption is intimately tied to the concept of label shift. Within the context of unsupervised transfer learning for classification under label shift, the estimation of the label distribution (or class proportions) of the target data, as well as the distribution shift function between the target and source domains, represents a pivotal task. Broadly speaking, existing methodologies for this purpose can be categorized into two primary groups. The first category revolves around comparing the moments of the target data with equivalent expressions derived from the source data distribution and the label distribution of the target data. Notable examples include the maximum mean discrepancy-based method (Zhang *et al.*, 2013; Iyer *et al.*, 2014), the black box shift learning (BBSL) method, and the regularized learning under label shift (RLLS)

methods (Lipton *et al.*, 2018; Azizzadenesheli *et al.*, 2019). The second category encompasses the maximum likelihood label shift (MLLS) method (Saerens *et al.*, 2002; Alexandari *et al.*, 2020), which is an instance of the expectation-maximization (EM) algorithm (Dempster *et al.*, 1977). Garg *et al.* (2020) presented a unified framework that connects MLLS and BBSL, revealing that MLLS often surpasses BBSL and RLLS in performance. Additionally, Jain *et al.* (2016) investigated the same problem, albeit with source data that can be considered unlabeled.

Another crucial task is the construction of valid classifiers for the target domain, as explored in (Saerens *et al.*, 2002; Azizzadenesheli *et al.*, 2019; Maity *et al.*, 2022). Two predominant approaches include weighted empirical risk minimization (Lipton *et al.*, 2018; Azizzadenesheli *et al.*, 2019) and the plugging-in method (in conjunction with the Bayes classifier) (Maity *et al.*, 2022). Many existing studies presuppose the availability of a classification model or the conditional distribution of  $Y$  given  $X$  for the source data, which can be estimated using an artificial neural network, logistic regression, or kernel-based methods. However, these studies either lack theoretical guarantees (Saerens *et al.*, 2002; Alexandari *et al.*, 2020) or may exhibit suboptimal finite-sample performance (Maity *et al.*, 2022). Recently, under the label shift assumption, Lee *et al.* (2024) developed a doubly flexible estimation method for the target population within the framework of semiparametric efficiency theory. Nonetheless, their focus was on parameter estimation rather than classification. Most importantly, the existing results derived under the label shift assumption may not be applicable under the GCS assumption.

Another closely related distribution shift assumption to GCS is posterior drift, which signifies that the conditional probabilities of labels given features differ between the source and target domains. Existing research on transfer learning under posterior drift has been conducted under specific similarity assumptions (Cai and Wei, 2021; Reeve *et al.*, 2021; Maity *et al.*, 2024). Our GCS bears a strong resemblance to the linear adjustment model proposed by Maity *et al.* (2024), which represents a particular similarity assumption between the source and target domains. However, unlike the current paper, where the observed target data are unlabeled, these prior works necessitate access to target labels and do not grapple with identifiability challenges. Consequently, they are not applicable to our specific setting.

A pivotal component of our methodology is the deep neural network (DNN), which has driven substantial advancements over the past few decades (Szegedy *et al.*, 2015; Sarikaya *et al.*, 2014; Miao and Miao, 2018). Mathematically, a DNN is a composite function comprising simplistic functions layered in multiple tiers, imparting it with the remarkable ability to approximate complex relationships with high precision. Theoretical analyses have demonstrated its capacity to approximate a wide spectrum of functions with specific structures, such as composite smooth functions (Bauer and Kohler, 2019), functions in Sobolev spaces (Yarotsky, 2017), and non-smooth functions (Imaizumi and Fukumizu, 2019). Owing to its formidable approximation power, DNNs have garnered significant attention in numerous fields, including nonparametric regression (Schmidt-Hieber, 2020; Jiao *et al.*, 2023), survival analysis (Zhong *et al.*, 2022), quantile regression (Shen *et al.*, 2024), and causal inference (Chen *et al.*, 2024), among others. In this paper, we utilize DNNs to transfer knowledge between domains in an unsupervised setting under the GCS model, representing a variant of deep transfer learning (Tan *et al.*, 2018; Iman *et al.*, 2023).

## 1.4 Organization

The organization of the remainder of this paper is as follows. Section 2 establishes the identifiability conditions for the target distribution within the framework of our GCS model and formally introduces a nonparametric setting for classification. In Section 3, we present the proposed DNN estimator for the classification function of the source data, along with a pseudo-maximum likelihood estimator for the class proportions of the target data. By integrating these two estimators, we derive the proposed classifier for the target data. Section 4 undertakes a comprehensive examination of the large-sample properties of the proposed estimators and classifier, encompassing concentration bounds, upper bounds in terms of excess risk, and minimax optimality. Sections 5 and 6 provide a detailed simulation study and a real data analysis, respectively. Finally, Section 7 concludes with some remarks. For clarity and ease of reading, all technical proofs have been deferred to the supplementary material.

## 2 Identifiability and nonparametric classification

Without loss of generality, we assume the label space  $\mathcal{Y}$  is given by  $\{1, 2, \dots, k\}$  for  $k \geq 2$ , and the feature space  $\mathcal{X}$  is  $[0, 1]^d$ . Our objective is to develop a valid classifier using a deep neural network (DNN) for the unsupervised target data, based on the observed data specified in (1), under the GCS assumption in (2).

### 2.1 Notation

In this paper, we adopt a nonparametric assumption concerning the classification of the target data. To facilitate our discussion, we introduce the necessary notation. Let  $P$  and  $Q$  represent the probability measures induced by  $P_{(X,Y)}$  and  $Q_{(X,Y)}$ , respectively, and let  $P_X$  and  $Q_X$  denote the distribution functions or probability measures of  $X$  in the source and target domains, respectively. We use  $\mathcal{P}$  to denote the pair of source and target distributions  $(P_{(X,Y)}, Q_{(X,Y)})$  and define  $[k] = \{1, 2, \dots, k\}$ . For  $l \in [k]$ , let  $\pi_{Q,l} = Q(Y = l)$ ,  $\pi_{P,l} = P(Y = l)$ ,  $\eta_{Q,l}(x) = Q(Y = l | X = x)$ ,  $\eta_{P,l}(x) = P(Y = l | X = x)$ ,  $f_l(x) = Q_{X|Y}(x | l)$  and  $\alpha_l = \log(\pi_{P,k}/\pi_{P,l})$ . Additionally, we define  $\boldsymbol{\eta}_P(x) = (\eta_{P,1}(x), \dots, \eta_{P,k-1}(x))^\top$ ,  $\boldsymbol{\eta}_Q(x) = (\eta_{Q,1}(x), \dots, \eta_{Q,k-1}(x))^\top$  and  $\boldsymbol{\pi}_Q = (\pi_{Q,1}, \dots, \pi_{Q,k-1})^\top$ .

We use  $\mathcal{D} = \{(X_1^P, Y_1^P), \dots, (X_{n_P}^P, Y_{n_P}^P); X_1^Q, \dots, X_{n_Q}^Q\}$  to denote the observed data (1) in  $\mathcal{S} = (\mathcal{X} \times \mathcal{Y})^{n_P} \times \mathcal{X}^{n_Q}$ , and use  $\mathcal{H} = \{\tilde{h} : \mathcal{X} \mapsto \mathcal{Y}\}$  to denote the set of all classifiers on  $\mathcal{X}$ . For any classifier  $\tilde{h} \in \mathcal{H}$ , its excess-risk is defined as

$$\mathcal{E}_Q(\tilde{h}) = Q(Y \neq \tilde{h}(X)) - Q(Y \neq f_Q^*(X)), \quad (3)$$

where  $f_Q^*(X) = \operatorname{argmax}_{l \in \mathcal{Y}} \eta_{Q,l}(X)$  is the Bayes classifier for the target data.

Let  $\|\cdot\|$  denote the standard Euclidean norm. We employ  $\lambda_{\min}(\cdot)$  to represent the minimal eigenvalue of a matrix, and use  $\|\cdot\|_\infty$  to signify the supremum norm of matrices, vectors or functions. Furthermore, let  $\mathbb{N}$ ,  $\mathbb{N}_+$  and  $\mathbb{R}_+$  denote the sets of natural numbers, positive natural numbers, and positive real numbers, respectively. For any distribution or probability measure  $M$  and any function  $f$  defined on  $\mathcal{X}$ ,  $\mathbb{E}_M[f(X)]$  denotes the expectation value of  $f(X)$  with respect to  $X \sim M$ . For any values  $a$  and  $b$ , let  $a \vee b := \max\{a, b\}$  and  $a \wedge b := \min\{a, b\}$ , where  $:=$  indicates “defined as”.



## 2.2 Identifiability

Because the target data lack labels, the target distribution  $Q_{(X,Y)}$  and  $h(\cdot)$  in (2) may not be identifiable without incorporating additional assumptions. Therefore, it is crucial to examine the issue of identifiability prior to presenting our learning algorithm.

**Assumption 2.** (i) For the function class  $\mathcal{H}$  in Assumption 1 and any  $\tilde{h} \in \mathcal{H}$ ,  $\tilde{h}(x) \cdot P_{X|Y}(x | 1), \dots, \tilde{h}(x) \cdot P_{X|Y}(x | k)$  are nondegenerate probability density or mass functions. (ii) As functions of  $x$  on  $\mathcal{X}$ ,  $P_{X|Y}(x | 1), \dots, P_{X|Y}(x | k)$  are linearly independent. (iii)  $\pi_{Q,i} > 0$  for all  $1 \leq i \leq k$ .

Assumption 2(i)-(ii) are relatively straightforward. Under Assumption 1, the constant function 1 belongs to the function class  $\mathcal{H}$ . Then, Assumption 2(i) implicitly assumes that the conditional probability density or mass functions  $P_{X|Y}(x | 1), \dots, P_{X|Y}(x | k)$  are all nondegenerate. In Assumption 2 (iii), we impose the condition that  $\pi_{Q,i} > 0$  for all  $1 \leq i \leq k$  to ensure that the target distribution has the same support as the source distribution.

We have discovered that the combination of Assumptions 1 and 2 constitutes a sufficient condition for the identifiability of  $Q_{(X,Y)}$  and  $h(\cdot)$ . This finding is formally articulated in the following lemma.

**Lemma 1.** Under Assumptions 1 and 2, the target distribution  $Q_{(X,Y)}$  and the function  $h(\cdot)$  in model (2) are identifiable from the data in (1).

## 2.3 Nonparametric setting for classification

Before presenting our nonparametric setting for classification, we introduce two types of function classes that play crucial roles in the construction of our classifier. The first type is Hölder classes, which are frequently utilized in nonparametric regression and machine learning (Stone, 1982; Cai and Wei, 2021; Maity *et al.*, 2022; Reeve *et al.*, 2021).

**Definition 1** (Hölder classes). Let  $a$  and  $M$  be positive constants, and let  $\mathbb{D} \subset \mathbb{R}^d$ . The following class

$$\mathcal{H}_d^a(\mathbb{D}, M) = \left\{ f : \mathbb{D} \mapsto \mathbb{R} \left| \sum_{\lambda: |\lambda| < a} \|\partial^\lambda f\|_\infty + \sum_{\lambda: |\lambda| = [a]} \sup_{x, y \in \mathbb{D}, x \neq y} \frac{|\partial^\lambda f(x) - \partial^\lambda f(y)|}{\|x - y\|_\infty^{a - [a]}} \leq M \right. \right\}$$

is called a Hölder class of smooth functions. Here,  $\lambda = (\lambda_1, \dots, \lambda_d)$  with  $\lambda_i$  being nonnegative integers,  $|\lambda| = \sum_{i=1}^d \lambda_i$ ,  $\partial^\lambda := \partial^{\lambda_1} \dots \partial^{\lambda_d}$ , and  $[a]$  denotes the largest integer strictly smaller than  $a$ .

A function within the class  $\mathcal{H}_d^a(\mathbb{D}, M)$  possesses a Hölder smoothness index of  $a$ . If a conditional mean regression function belongs to  $\mathcal{H}_d^a(\mathbb{D}, M)$ , Stone (1982) revealed that the optimal minimax rate of convergence for estimating it is  $n_P^{-\frac{a}{2a+d}}$ . In numerous transfer learning studies, specific nonparametric components of the underlying problem are presumed to belong to a Hölder class, such as  $\mathcal{H}_d^a(\mathbb{D}, M)$  (Cai and Wei, 2021; Maity *et al.*, 2022; Reeve *et al.*, 2021). Under this assumption, the minimax optimal rate of convergence for the classifier on the target data, in terms of excess-risk, hinges on the smoothness index  $a$  and the dimension  $d$ . For instance, this rate may be  $n_P^{-\frac{a(1+c_2)}{2c_1a+d}} + n_Q^{-\frac{a(1+c_2)}{2a+d}}$  for some positive constants  $c_1$  and  $c_2$  (Cai and Wei, 2021). When the dimension  $d$  is substantial, this rate can be extremely slow. To mitigate this curse of dimensionality, we consider another type of function class.

**Definition 2** (Composite smoothness function class (Schmidt-Hieber, 2020)). *Let  $q \in \mathbb{N}$ ,  $M \geq 1$ ,  $\theta = (\theta_0, \dots, \theta_q) \in \mathbb{R}_+^{q+1}$  and  $\mathbf{k} = (k_0, \dots, k_{q+1}) \in \mathbb{N}_+^{q+2}$ , and  $\tilde{\mathbf{k}} = (\tilde{k}_0, \dots, \tilde{k}_q) \in \mathbb{N}_+^{q+1}$  with  $\tilde{k}_j \leq k_j$ ,  $j = 0, \dots, q$ . The following class*

$$\mathcal{G}(q, \theta, \mathbf{k}, \tilde{\mathbf{k}}, M) = \left\{ f = g_q \circ \dots \circ g_0 \left| \begin{array}{l} g_i = (g_{ij})_j : [a_i, b_i]^{k_i} \rightarrow [a_{i+1}, b_{i+1}]^{k_{i+1}}, \\ g_{ij} \in \mathcal{H}_{\tilde{k}_i}^{\theta_i}([a_i, b_i]^{\tilde{k}_i}, M), \text{ for some } |a_i|, |b_i| \leq M \end{array} \right. \right\}$$

with  $k_0 = d$ ,  $k_{q+1} = 1$ ,  $a_0 = 0$ ,  $b_0 = 1$ , and  $f \circ g = f(g(\cdot))$  is called a composite smoothness function class.

For a constant vector  $\theta$ , let  $\gamma_{n_P} = \max_{i=0, \dots, q} n_P^{-\tilde{\theta}_i / (2\tilde{\theta}_i + \tilde{k}_i)}$ , where  $\tilde{\theta}_i = \theta_i \prod_{j=i+1}^q (\theta_j \wedge 1)$ . Let  $i^* \in \operatorname{argmin}_{i \in \{0, \dots, q\}} \tilde{\theta}_i / (2\tilde{\theta}_i + \tilde{k}_i)$ . To some extent,  $\tilde{k}_{i^*}$  characterizes the intrinsic dimension of the function class  $\mathcal{G}(q, \theta, \mathbf{k}, \tilde{\mathbf{k}}, M)$ . In this paper, we assume that after an equivalence transformation, the ideal classification function of the source domain belongs to a composite smoothness function class. We uncover that under this assumption, the convergence rate of our estimator (See Section 3.1) for the classification function hinges upon the intrinsic dimension of the classification function. Intuitively, the structure of the composite functions within  $\mathcal{G}(q, \theta, \mathbf{k}, \tilde{\mathbf{k}}, M)$  bears resemblance to the multi-layer perceptron structure of neural networks, which endows the resultant

estimator with relatively smaller approximation errors or a faster convergence rate. Consequently, we anticipate that the proposed methodology can mitigate the curse of dimensionality when the classification function in the source domain exhibits a low-dimensional structure (Schmidt-Hieber, 2020; Zhong *et al.*, 2022).

With the aforementioned preparations in place, we impose the requirement that the distribution pair  $\mathcal{P}$  of interest must adhere to Assumption 3.

**Assumption 3.** *The distribution pair  $\mathcal{P}$  satisfies (i) Assumption 1 (the GCS assumption) holds to be true. (ii) There exists a group of parameters  $(q, \theta, \mathbf{k}, \tilde{\mathbf{k}}, M)$  such that  $\phi_k(\cdot) = 0$  and*

$$\eta_{P,l}(\cdot) = \frac{\exp\{\phi_l(\cdot)\}}{1 + \sum_{i=1}^{k-1} \exp\{\phi_i(\cdot)\}}, \quad \phi_l(\cdot) \in \mathcal{G}(q, \theta, \mathbf{k}, \tilde{\mathbf{k}}, M), \quad l \in [k-1]. \quad (4)$$

*(iii) There exists  $\tilde{c} > 1$  such that  $dQ_X(x)/dP_X(x) \leq \tilde{c}$  for all  $x \in \mathcal{X}$ . (iv) Assumption 2 is satisfied.*

Assumption 3 (iii) is a weaker version of the strong density assumptions in Definition 4 of Cai and Wei (2021). Given a set of parameters  $(h, q, \theta, \mathbf{k}, \tilde{\mathbf{k}}, M, \tilde{c})$ , we denote the class of distribution pairs  $\mathcal{P}$  that satisfy Assumption 3 as  $\mathcal{P}^*(h, q, \theta, \mathbf{k}, \tilde{\mathbf{k}}, M, \tilde{c})$ . For brevity, we may also refer to this class as  $\mathcal{P}^*$ . To signify the true value of parameter, we append a suffix 0 to it; for instance,  $\pi_Q^0$  represents the true value of  $\pi_Q$ .

### 3 Classification with deep transfer learning

This section introduces the proposed nonparametric classifier that leverages deep transfer learning. Initially, we train a *Deep Neural Network* (DNN) estimator, denoted as  $\hat{\eta}_P$ , for  $\eta_P$ . Subsequently, we estimate  $\pi_Q$  using a pseudo maximum likelihood estimator, named  $\hat{\pi}_Q$ . The classifier is constructed by combining  $\hat{\eta}_P$  and  $\hat{\pi}_Q$  through Bayes' formula. A notable advantage of our method is its innovative circumvention of the necessity to estimate the unknown function  $h(\cdot)$  in the GCS model (2).

#### 3.1 DNN estimator for $\eta_P$

Since  $\eta_P$  represents the regression of  $Y$  on  $X$  under the source data distribution and the source data are fully available,  $\eta_P$  is nonparametrically identifiable and

can be consistently estimated using any nonparametric regression technique. Within the framework of model (4), estimating  $\eta_P$  is equivalent to estimating  $\phi(\cdot) = (\phi_1(\cdot), \dots, \phi_{k-1}(\cdot))^\top$ . Given its remarkable flexibility and widespread popularity, we propose using a DNN to estimate  $\phi(\cdot)$  and consequently  $\eta_P$ .

Let  $K \in \mathbb{N}_+$  and  $\mathbf{p} = (p_0, \dots, p_K, p_{K+1}) \in \mathbb{N}_+^{K+2}$ . A  $(K+1)$ -layer DNN with layer width specified by  $\mathbf{p}$  is a composition function  $g : \mathbb{R}^{p_0} \mapsto \mathbb{R}^{p_{K+1}}$  defined recursively as follows:

$$g(x) = W_K g_K(x), g_K(x) = \sigma(W_{K-1} g_{K-1}(x) + \mu_{K-1}), \dots, g_1(x) = \sigma(W_0 x + \mu_0). \quad (5)$$

Here, the matrices  $W_j \in \mathbb{R}^{p_{j+1} \times p_j}$  for  $j = 0, \dots, K$ , and the vectors  $\mu_l \in \mathbb{R}^{p_{l+1}}$  for  $l = 0, \dots, K-1$ , constitute the parameters of the DNN. The activation function  $\sigma$  operates component-wise, meaning that  $g_j = (g_{j1}, \dots, g_{jp_j})^\top$  maps from  $\mathbb{R}^{p_{j-1}}$  to  $\mathbb{R}^{p_j}$  for each  $j = 1, \dots, K$ . The parameter  $K$  represents the depth of the DNN, while  $\mathbf{p}$  enumerates the width of each layer ( $p_0$  corresponds to the dimension of the input variable,  $p_1, \dots, p_K$  denote the dimensions of the  $K$  hidden layers, and  $p_{K+1}$  specifies the dimension of the output layer). For illustrative purpose, Figure 3.1 depicts a three-layers DNN with  $K = 2$  and  $\mathbf{p} = (4, 3, 3, 1)$ .

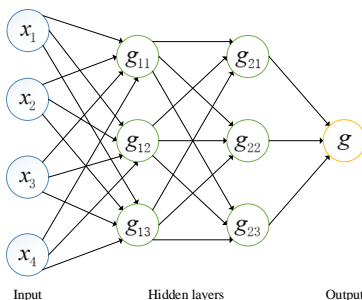


Figure 1: A three layers deep neural network with  $K = 2$  and  $\mathbf{p} = (4, 3, 3, 1)$ .

The activation function  $\sigma$  must be selected beforehand. While sigmoidal activation functions were commonly used in neural networks, the nonsigmoidal rectified linear unit (ReLU), denoted as  $x \vee 0$ , offers computational advantages for DNN (Schmidt-Hieber, 2020). In terms of statistical performance, the ReLU has been found to outperform sigmoidal activation functions for classification problems (Glorot *et al.*, 2011; Pedamonti, 2018). In this paper, we adopt the ReLU activation function and consistently set  $p_0 = d$  and  $p_{K+1} = 1$ .

A fully-connected, deep feedforward network often suffers from overfitting. To address this challenge, we consider a sparsely connected network approach (Han *et al.*, 2015; Srinivas *et al.*, 2017; Schmidt-Hieber, 2020; Zhong *et al.*, 2022). Given  $K, s \in \mathbb{N}_+$ ,  $\mathbf{p} \in \mathbb{N}_+^{K+2}$  and  $D > 0$ , we define a class of sparse neural networks as follows:

$$\mathcal{F}(K, s, \mathbf{p}, D) = \left\{ g \mid g \text{ is a } (K+1)\text{-layer DNN with width } \mathbf{p} \text{ such that } \|g\|_\infty \leq D, \right. \\ \left. \sum_{i=0}^K (\|W_i\|_0 + \|\mu_i\|_0) \leq s, \max_{j \in \{0, 1, \dots, K\}} \{\|W_j\|_\infty, \|\mu_j\|_\infty\} \leq 1 \right\},$$

where  $\mu_K$  is a  $p_{K+1}$ -dimensional zero and  $\|\cdot\|_0$  denotes the number of nonzeros entries of a matrix or vector. We model  $\phi = (\phi_1, \dots, \phi_{k-1})^\top$  using a sparsely connected network, specifically,  $\phi \in \{\mathcal{F}(K, s, \mathbf{p}, D)\}^{k-1}$ .

Under the model specified in (4), we propose to estimate  $\phi$  using the following nonparametric maximum likelihood estimator

$$\hat{\phi} = \underset{\phi \in \{\mathcal{F}(K, s, \mathbf{p}, D)\}^{k-1}}{\operatorname{argmax}} \sum_{i=1}^{n_P} \left\{ \sum_{l=1}^{k-1} I(Y_i^P = l) \phi_l(X_i^P) - \log \left( 1 + \sum_{j=1}^{k-1} \exp\{\phi_j(X_i^P)\} \right) \right\}, \quad (6)$$

where  $\hat{\phi}(\cdot) = (\hat{\phi}_1(\cdot), \dots, \hat{\phi}_{k-1}(\cdot))^\top$  and  $I(A)$  denotes the indicator function of an event  $A$ . Once  $\hat{\phi}$  is obtained, we can construct a DNN estimator for  $\eta_P^0$  by simply plugging in the estimate, i.e.  $\hat{\eta}_P(\cdot) := (\hat{\eta}_{P,1}(\cdot), \dots, \hat{\eta}_{P,k-1}(\cdot))^\top$ , where

$$\hat{\eta}_{P,l}(x) = \frac{\exp\{\hat{\phi}_l(x)\}}{1 + \sum_{j=1}^{k-1} \exp\{\hat{\phi}_j(x)\}}, \quad l \in [k-1], \quad x \in \mathcal{X}.$$

The depth  $K$  and the width vector  $\mathbf{p}$  govern both the complexity and flexibility of the neural networks in  $\mathcal{F}(K, s, \mathbf{p}, D)$ , as well as those inherent in the conditional probabilities  $\hat{\eta}_P(x)$ . These hyperparameters can be selected using cross-validation or held-out validation in practical applications.

### 3.2 Pseudo maximum likelihood estimator of $\pi_Q$

In the second step, we propose to estimate  $\pi_Q$  by a pseudo maximum likelihood estimation method. For a generic unlabeled observation  $X^Q$ , it follows a  $k$ -component mixture model given by  $\sum_{j=1}^k \pi_{Q,j} f_j(x)$ . Under the GCS model (2), for  $l \in [k-1]$ , we

have

$$\begin{aligned} \frac{f_l(x)}{f_k(x)} &= \frac{Q_{X|Y}(x | l)}{Q_{X|Y}(x | k)} = \frac{P_{X|Y}(x | l) \cdot h(x)}{P_{X|Y}(x | k) \cdot h(x)} \\ &= \frac{P(Y = l | X = x) / P(Y = l)}{P(Y = k | X = x) / P(Y = k)} = \frac{\eta_{P,l}(x) \pi_{P,k}}{\eta_{P,k}(x) \pi_{P,l}}. \end{aligned} \quad (7)$$

Given model (4), since  $\phi_k(x) \equiv 0$ , we obtain  $f_l(x) = \exp\{\alpha_l + \phi_l(x)\} f_k(x)$  with  $\alpha_l = \log(\pi_{P,k} / \pi_{P,l})$ , for  $l \in [k]$ . Therefore, the density of  $X^Q$  can be expressed as

$$f_k(x) \sum_{j=1}^k \pi_{Q,j} \exp\{\alpha_j + \phi_j(x)\} = f_k(x) \left[ \sum_{j=1}^{k-1} \pi_{Q,j} \exp\{\alpha_j + \phi_j(x)\} + \left(1 - \sum_{l=1}^{k-1} \pi_{Q,l}\right) \right].$$

This implies that the log-likelihood contribution of  $X^Q$  is  $\log f_k(X^Q) + \ell_Q(X^Q; \boldsymbol{\alpha}, \boldsymbol{\phi}, \boldsymbol{\pi}_Q)$ , where  $\boldsymbol{\alpha} = (\alpha_1, \dots, \alpha_{k-1})^\top$  and

$$\ell_Q(X^Q; \boldsymbol{\alpha}, \boldsymbol{\phi}, \boldsymbol{\pi}_Q) = \log \left[ \sum_{l=1}^{k-1} \pi_{Q,l} \exp(\alpha_l + \phi_l(X^Q)) + \left(1 - \sum_{j=1}^{k-1} \pi_{Q,j}\right) \right].$$

Since the term  $\log f_k(X^Q)$  does not involve  $\pi_{Q,l}$ , we can ignore it and consider  $\ell_Q(X^Q; \boldsymbol{\alpha}, \boldsymbol{\phi}, \boldsymbol{\pi}_Q)$  as the likelihood contribution of  $X^Q$ .

The likelihood function,  $\sum_{i=1}^{n_Q} \ell_Q(X_i^Q; \boldsymbol{\alpha}, \boldsymbol{\phi}, \boldsymbol{\pi}_Q)$ , is dependent not solely on  $\boldsymbol{\pi}_Q$ , but also on  $\boldsymbol{\phi}$  and  $\boldsymbol{\alpha}$ . In the preceding subsection, we have devised a DNN estimator,  $\hat{\boldsymbol{\phi}}$ , for  $\boldsymbol{\phi}$ . A straightforward estimator for  $\boldsymbol{\alpha}$  is derived as follows:  $\hat{\boldsymbol{\alpha}} = (\log(\hat{\pi}_{P,k} / \hat{\pi}_{P,1}), \dots, \log(\hat{\pi}_{P,k} / \hat{\pi}_{P,k-1}))^\top$ , where  $\hat{\pi}_{P,l} = (1/n_P) \sum_{j=1}^{n_P} I(Y_j^P = l)$  for  $l \in [k]$ . Substituting  $(\hat{\boldsymbol{\alpha}}, \hat{\boldsymbol{\phi}})$  for  $(\boldsymbol{\alpha}, \boldsymbol{\phi})$ , we obtain a pseudo-likelihood function of  $\boldsymbol{\pi}_Q$ , i.e.  $\sum_{j=1}^{n_Q} \ell_Q(X_j^Q; \hat{\boldsymbol{\alpha}}, \hat{\boldsymbol{\phi}}, \boldsymbol{\pi}_Q)$ . To estimate  $\boldsymbol{\pi}_Q$ , we propose utilizing the pseudo maximum likelihood estimator (PMLE),

$$\hat{\boldsymbol{\pi}}_Q = \operatorname{argmax}_{\boldsymbol{\pi}_Q \in \Pi} \sum_{j=1}^{n_Q} \ell_Q(X_j^Q; \hat{\boldsymbol{\alpha}}, \hat{\boldsymbol{\phi}}, \boldsymbol{\pi}_Q), \quad (8)$$

where  $\Pi := \{\boldsymbol{\pi}_Q | \pi_{Q,l} \in [0, 1]^{k-1}, 1 - \boldsymbol{\pi}_Q^\top \mathbf{1}_{k-1} \geq 0\}$ , and  $\mathbf{1}_{k-1}$  denotes a  $(k-1)$ -dimensional vector of 1. This estimation procedure for  $\boldsymbol{\pi}_Q$  is exceptionally versatile and adaptable as it works once reasonable estimates of the density ratios  $\{f_l(\cdot) / f_k(\cdot)\}_{l=1}^{k-1}$  or equivalently  $\{P_{X|Y}(x | l) / P_{X|Y}(x | k)\}_{l=1}^{k-1}$  are available.

### 3.3 The proposed classifier

Ideally the optimal classifier for the target domain in terms of excess-risk is the Bayes classifier, defined as  $f_Q^*(x) = \arg \max_{y \in [k]} \eta_{Q,y}(x)$ . To estimate this classifier,

we propose estimating the regression function  $\eta_{Q,y}(x)$ . For  $y \in [k]$ , Bayes's formula dictates that  $\eta_{Q,y}(x) = \pi_{Q,y}Q_{X|Y}(x | y) / \sum_{j=1}^k \pi_{Q,j}Q_{X|Y}(x | j)$ . By leveraging the GCS model (2), we can further derive

$$\eta_{Q,l}(x) = \frac{\pi_{Q,l}P_{X|Y}(x | l) \cdot h(x)}{\sum_{j=1}^k \pi_{Q,j}P_{X|Y}(x | j) \cdot h(x)} = \frac{\eta_{P,l}(x)\pi_{Q,l}/\pi_{P,l}}{\sum_{j=1}^k \eta_{P,j}(x)\pi_{Q,j}/\pi_{P,j}}, \quad (9)$$

where the last equality is a consequence of (7).

By substituting  $\hat{\eta}_{P,j}(x)$ ,  $\hat{\pi}_{Q,j}$  and  $\hat{\pi}_{P,j}$  into equation (9), we have the following plug-in estimators

$$\hat{\eta}_{Q,l}(x) = \frac{\hat{\eta}_{P,l}(x)\hat{\pi}_{Q,l}/\hat{\pi}_{P,l}}{\sum_{j=1}^k \hat{\eta}_{P,j}(x)\hat{\pi}_{Q,j}/\hat{\pi}_{P,j}}, \quad l = 1, 2, \dots, k-1. \quad (10)$$

Ultimately, our proposed classifier for unlabelled target data is given by

$$\hat{f}(x) = \operatorname{argmax}_{l \in [k]} \hat{\eta}_{Q,l}(x) = \operatorname{argmax}_{l \in [k]} \frac{\hat{\pi}_{Q,l}}{\hat{\pi}_{P,l}} \hat{\eta}_{P,l}(x). \quad (11)$$

A notable advantage of our classifier is that it circumvents the problem of estimating the function  $h(\cdot)$  in the GCS model (2). This is because  $h(\cdot)$  appears in both the numerator and the denominator of equality (9), resulting in its cancellation. Consequently, it is unnecessary to estimate  $h(\cdot)$  in (10) although  $h(\cdot)$  is theoretically identifiable (as stated in Lemma 1) and can be consistently estimated.

## 4 Asymptotics

This section investigates the asymptotic properties of the proposed estimators  $\hat{\eta}_P$  and  $\hat{\pi}_Q$ , as well as the proposed classifier  $\hat{f}(x)$  when utilized with target data.

### 4.1 Concentration bounds for $\hat{\eta}_P$ and $\hat{\pi}_Q$

We commence by presenting concentration bounds for the DNN estimator  $\hat{\eta}_P$  of  $\eta_P$  and the PMLE  $\hat{\pi}_Q$  of  $\pi_Q$ . To facilitate the ensuing discussion, we introduce additional notations. For any two sequences  $(a_{n_P})_{n_P}$  and  $(b_{n_P})_{n_P}$ , we denote  $a_{n_P} \lesssim b_{n_P}$  if there exists a positive constant  $C$  such that  $a_{n_P} \leq Cb_{n_P}$  for all  $n_P$ . The notation  $a_{n_P} \asymp b_{n_P}$  signifies that both  $a_{n_P} \lesssim b_{n_P}$  and  $b_{n_P} \lesssim a_{n_P}$ . We define  $\boldsymbol{\xi}^0(x) = (\alpha_1^0 + \phi_1^0(x), \dots, \alpha_{k-1}^0 +$

$\phi_{k-1}^0(x)^\top$  and introduce  $\boldsymbol{\chi} = \mathbb{E}_{Q_X}[(\exp\{\boldsymbol{\xi}^0(X)\} - \mathbf{1}_{k-1})^{\otimes 2} / (\mathbf{1}_{k-1}^\top \exp\{\boldsymbol{\xi}^0(X)\} + 1)^2]$ , where  $A^{\otimes 2} = AA^\top$  for any vector or matrix  $A$ . Furthermore, we denote  $c_\lambda = \lambda_{\min}(\boldsymbol{\chi})$ . Throughout our discussion,  $\mathbb{E}_{\mathcal{D}}$  will be used to represent the expectation taken with respect to the randomness of  $\mathcal{D}$ .

Drawing inspiration from Schmidt-Hieber (2020) and Zhong *et al.* (2022), we impose the following assumption pertaining to the network architectures of  $\mathcal{F}(K, s, \mathbf{p}, D)$ .

**Assumption 4.** *The neural network  $\mathcal{F}(K, s, \mathbf{p}, D)$  satisfies (i)  $D \geq (M \vee 1)$ , (ii)  $\sum_{i=0}^q \log_2(4\tilde{k}_i \vee 4\theta_i) \log_2 n_P \leq K \lesssim \log n_P$ , (iii)  $n_P \gamma_{n_P}^2 \lesssim \min_{i \in [K]} p_i \leq \max_{i \in [K]} p_i \leq n_P$ , (iv)  $s \asymp n_P \gamma_{n_P}^2 \log n_P$ .*

For any function  $\mathbf{f}_1$  and  $\mathbf{f}_2$  from  $[0, 1]^d$  to  $\mathbb{R}^{k-1}$ , let  $d_P^2(\mathbf{f}_1, \mathbf{f}_2) = \mathbb{E}_{P_X}\{\|\mathbf{f}_1(X) - \mathbf{f}_2(X)\|^2\}$ . Theorem 1 establishes a concentration bound for the DNN estimator  $\hat{\boldsymbol{\eta}}_P$ .

**Theorem 1.** *Suppose the data  $\mathcal{D}$  is generated according to the distribution pair  $\mathcal{P}$ , and that Assumption 3 (ii) and Assumption 4 are satisfied. Then, for any  $\varepsilon \in (0, 1)$  and sufficiently large  $n_P$ , it holds with probability at least  $1 - \varepsilon$  that*

$$d_P(\hat{\boldsymbol{\eta}}_P, \boldsymbol{\eta}_P^0) \leq \zeta_1 \sqrt{\log\left(\frac{\zeta_2}{\varepsilon}\right)} \cdot \gamma_{n_P} \log^2 n_P,$$

where  $\zeta_1$  and  $\zeta_2$  are positive constants depending solely on  $M$ ,  $D$  and  $k$ .

According to Theorem 1, the convergence rate of our DNN estimator of  $\boldsymbol{\eta}_P$  is of the order  $\gamma_{n_P} \log^2 n_P$ , which hinges on the intrinsic dimension  $\tilde{k}_{i^*}$ . The convergence rate,  $\gamma_{n_P} \log^2 n_P$ , aligns with that of the estimator presented in Schmidt-Hieber (2020) in the realm of nonparametric regression with Gaussian errors, under the composite smoothness assumption on the true regression function. When  $k = 2$ , the classification function  $\eta_{P,1}$  can be regarded as the propensity score function in causal inference and missing data problems. It serves as a crucial component in the widely-used augmented inverse probability weighting (Robins *et al.*, 1994, AIPW) and double machine learning methods (Chernozhukov *et al.*, 2018, DML). Along with other conditions, the convergence rate result of our DNN estimator  $\hat{\eta}_{P,1}$  presented in Theorem 1 can be used to verify whether the AIPW and DNN methods achieve the asymptotically semiparametric efficiency lower bound (Chernozhukov *et al.*, 2018).



To derive a concentration bound for  $\hat{\pi}_Q$ , we necessitate an additional restriction on the neural networks within  $\mathcal{F}(K, s, \mathbf{p}, D)$ . Specifically, the constant  $s$  governs the number of active parameters or the sparsity of these networks.

**Assumption 5.**  $s = o(n_Q \gamma_{n_P} + \sqrt{n_Q} \log^{-3} n_P)$  as  $n_P$  and  $n_Q$  go to infinity.

Assumption 5 stipulates that the sparsity of the neural network should not increase too rapidly. Provided that this assumption is met, Theorem 2 furnishes a concentration bound for the proposed PMLE  $\hat{\pi}_Q$ , which represents a novel contribution to the existing literature.

**Theorem 2.** *Suppose that the data  $\mathcal{D}$  is generated according to the distribution pair  $\mathcal{P}$ , and that Assumptions 3–5 are satisfied. Then, for any  $\varepsilon \in (0, 1)$  and sufficiently large  $n_P$  and  $n_Q$ , it holds with probability at least  $1 - \varepsilon$  that*

$$\|\hat{\pi}_Q - \pi_Q^0\| \leq \zeta_3 \sqrt{\log\left(\frac{\zeta_4}{\varepsilon}\right)} \cdot (\gamma_{n_P} \log^2 n_P + n_Q^{-1/2}), \quad (12)$$

where  $\zeta_3$  and  $\zeta_4$  are some positive constants depending solely on  $\tilde{c}$ ,  $M$ ,  $D$ ,  $k$  and  $c_\lambda$ .

Theorem 2 suggests, in broad sense, that the convergence rate of our class proportion estimator is of the order  $(\gamma_{n_P} \log^2 n_P + n_Q^{-1/2})$ . When the size of the target data  $n_Q$  is substantial, the term  $\gamma_{n_P} \log^2 n_P$  becomes the dominant factor, whereas for smaller  $n_Q$ , the term  $n_Q^{-1/2}$  prevails. This finding presents a more intuitive and streamline form compared to the result in Iyer *et al.* (2014) [e.g., Theorem 1]. Theorem 2 indicates that the convergence rate of  $\hat{\pi}_{Q,l}$  is no faster than  $n_P^{-1/2}$ . Because the convergence rate of  $\hat{\pi}_{P,l}$  is  $n_P^{-1/2}$ , it also indicates that the estimate  $\hat{\pi}_{Q,l}/\hat{\pi}_{P,l}$  has the same convergence rate as  $\hat{\pi}_{Q,l}$ . This convergence rate establishes a theoretical cornerstone for deriving the generalization error bound of the minimizer of the weighted empirical risk under label shift (Azizzadenesheli *et al.*, 2019). More importantly, the results presented in Theorems 1–2 establish the groundwork for achieving the minimax optimal convergence rate of our proposed classifier in terms of excess-risk.

## 4.2 Minimax optimality of the proposed classifier

We initially derive an upper bound for the excess-risk  $\mathcal{E}_Q(\hat{f})$  of the proposed classifier  $\hat{f}(\cdot)$ , as defined in (11).

**Theorem 3.** *Suppose that the data  $\mathcal{D}$  is generated according to the distribution pair  $\mathcal{P}$ , and that Assumptions 3–5 are satisfied. Then, for any  $\varepsilon \in (0, 1)$  and sufficiently large  $n_P$  and  $n_Q$ , it holds with probability at least  $1 - \varepsilon$  that*

$$\mathcal{E}_Q(\hat{f}) \leq \zeta_5 \sqrt{\log\left(\frac{\zeta_6}{\varepsilon}\right)} \cdot \left(\gamma_{n_P} \log^2 n_P + n_Q^{-1/2}\right), \quad (13)$$

where  $\zeta_5$  and  $\zeta_6$  are some positive constants depending solely on  $\tilde{c}$ ,  $M$ ,  $D$ ,  $k$  and  $c_\lambda$ .

Given that for a nonnegative random variable  $T$ ,  $\mathbb{E}T = \int_0^\infty P(T \geq t)dt$ , Theorem 3 implies

$$\mathbb{E}_{\mathcal{D}}\{\mathcal{E}_Q(\hat{f})\} \leq \sqrt{2\pi} \cdot \zeta_6 \zeta_5 \left(\gamma_{n_P} \log^2 n_P + n_Q^{-1/2}\right), \quad (14)$$

indicating that the expected excess-risk  $\mathbb{E}_{\mathcal{D}}\{\mathcal{E}_Q(\hat{f})\}$  shares the same asymptotic convergence rate  $(\gamma_{n_P} \log^2 n_P + n_Q^{-1/2})$  as the excess-risk  $\mathcal{E}_Q(\hat{f})$ .

Furthermore, Theorem 3 elucidates that the contributions of the source and target data to the convergence rate of the proposed classifier are  $\gamma_{n_P} \log^2 n_P$  and  $n_Q^{-1/2}$ , respectively. Notably, the converge rate of our classifier is independent of  $d$ , allowing the proposed method to alleviate the curse of dimensionality when the dimension  $d$  of  $X$  is high but the intrinsic dimension of the composite function  $\phi^0(\cdot)$  remains relatively low. To illustrate this, we present two examples showcasing the selection of  $\phi^0(\cdot)$  with low-dimensional structures.

**Example 1** (Generalized additive model, GAM (Horowitz and Mammen, 2007)). *Consider functions  $\phi_{1,j} : [0, 1] \mapsto [-M_0, M_0]$  for some  $M_0 > 0$  and  $1 \leq j \leq d$ , and  $\tilde{H}(\cdot) : \mathbb{R} \mapsto \mathbb{R}$ . Define  $\phi_1^0(x) = \tilde{H}(\sum_{j=1}^d \phi_{1,j}(x_{(j)}))$ , where  $x_{(j)}$  denotes the  $j$ -th component of  $x$  and  $d$  is a positive integer. If we take  $g_0(x) = (\phi_{1,1}(x_{(1)}), \dots, \phi_{1,d}(x_{(d)}))^\top$ ,  $g_1(x) = \sum_{j=1}^d x_{(j)}$  and  $g_2(\cdot) = \tilde{H}(\cdot)$ , then  $\phi_1^0(x) = g_2 \circ g_1 \circ g_0(x)$ . Assume that  $\phi_{1,j} \in \mathcal{H}_1^{\theta_0}([0, 1], M_0)$  for  $j \in [d]$  and some  $\theta_0 > 0$ , and  $\tilde{H} \in \mathcal{H}_1^{\theta_2}([-dM_0, dM_0], M_1)$  for some  $\theta_2 > 0$  and  $M_1 > 0$ . It is clear that  $g_1(\cdot) \in \mathcal{H}_d^{\theta_1}([-M_0, M_0]^d, dM_0 + 1)$  for any  $\theta_1 > 1$ . Therefore  $\phi_1^0 \in \mathcal{G}(2, (\theta_0, (\theta_0 \vee 2)d, \theta_2), (d, d, 1, 1), (1, d, 1), (dM_0 + 1) \vee M_1)$ . According to Theorem 3, the contribution of the source data to the convergence rate of  $\mathcal{E}_Q(\hat{f})$  is of the order  $(n_P^{-\frac{\theta_0(\theta_2 \wedge 1)}{2\theta_0(\theta_2 \wedge 1)+1}} + n_P^{-\frac{\theta_2}{2\theta_2+1}}) \log^2(n_P)$ . Here are some important observations:*

- When  $\theta_0 = \theta_2 \geq 1$ , the rate simplifies to  $n_P^{-\frac{\theta_2}{2\theta_2+1}} \log^2(n_P)$ , which, up to a logarithm factor, aligns with the rate in Theorem 2.1 of Horowitz and Mammen (2007) in the context of penalized nonparametric (generalized additive) regression.
- The GAM reduces to an additive model (Stone, 1985) when  $\tilde{H}$  is the identity function. In this situation, the convergence rate contribution of the source data is of the order  $n_P^{-\frac{\theta_0}{2\theta_0+1}} \log^2(n_P)$ , which, up to a logarithm factor, coincides with the optimal minimax rate in Corollary 1 of Stone (1985) for additive (mean) regression.
- When  $\phi_{1,j}$  is a linear function of  $x_{(j)}$  for  $j \in [d]$ , the GAM reduces to the single index model (Ichimura, 1993), and the convergence rate contribution of the source data is of the order  $n_P^{-\frac{\theta_2}{2\theta_2+1}} \log^2(n_P)$ , which, up to a logarithm factor, matches the optimal rate in Theorem 3 of Ma and He (2016) for single-index (quantile) regression.

In all three cases, the convergence rate is independent of the dimension  $d$  of  $X$ , which can be any positive integer. This underscores that the ability of our method to mitigate the curse-of-dimensionality.

**Example 2** (Generalized hierarchical interaction model (Kohler and Krzyżak, 2016)).

For a fixed positive integer  $d^* \in \mathbb{N}_+$  ( $d^* < d$ ), consider vectors  $\beta_i^1, \dots, \beta_i^{d^*} \in \mathbb{R}^d$  ( $i \in [d^*]$ ), functions  $\tilde{f}_1, \dots, \tilde{f}_{d^*} : \mathbb{R}^{d^*} \mapsto \mathbb{R}$  and a function  $\tilde{H} : \mathbb{R}^{d^*} \mapsto \mathbb{R}$  such that

$$\phi_1^0(x) = \tilde{H} \left( \tilde{f}_1(x), \dots, \tilde{f}_{d^*}(x) \right), \quad \tilde{f}_i(x) = \tilde{f}_i(x^\top \beta_i^1, \dots, x^\top \beta_i^{d^*}), \quad 1 \leq i \leq d^*.$$

Define the functions:  $g_0(x) = (x^\top \beta_1^1, \dots, x^\top \beta_1^{d^*}, \dots, x^\top \beta_{d^*}^1, \dots, x^\top \beta_{d^*}^{d^*})^\top$ ,  $g_1(t_1, \dots, t_{d^*}) = (\tilde{f}_1(t_1), \dots, \tilde{f}_{d^*}(t_{d^*}))^\top$ , and  $g_2(t) = \tilde{H}(t)$ , where  $t, t_1, \dots, t_{d^*}$  are  $d^*$ -dimensional vectors. Assume that  $\|\beta_i^j\| \leq M_0$  for all  $i, j \in [d^*]$  for some  $M_0 > 0$ . Consequently, for any  $\theta_0 > 1$ , the linear functions  $x^\top \beta_i^j$  belong to  $\mathcal{H}_d^{\theta_0}([0, 1]^d, dM_0)$ . Furthermore, suppose that  $\tilde{f}_1, \dots, \tilde{f}_{d^*}, \tilde{H}$  all belong to  $\mathcal{H}_{d^*}^\theta([-M_1, M_1]^{d^*}, M_1)$  for some  $\theta > 0$  and sufficiently large  $M_1$ . Then it follows that

$$\phi_1^0 \in \mathcal{G} \left( 2, ((\theta \vee 2)d / (\theta \wedge 1))^2, \theta, \theta \right), (d, (d^*)^2, d^*, 1), (d, d^*, d^*), M_1 \vee dM_0 \right).$$

According to Theorem 3, the contribution of the source data to the convergence rate of  $\mathcal{E}_Q(\hat{f})$  is of the order  $(n_P^{-\frac{\theta(\theta \wedge 1)}{2\theta(\theta \wedge 1) + d^*}} + n_P^{-\frac{\theta}{2\theta + d^*}}) \log^2(n_P)$ . When  $\theta \geq 1$ , the rate simplifies

to  $n_P^{-\frac{\theta}{2\theta+d^*}} \log^2(n_P)$ , which aligns with the rate in Theorem 1 of Bauer and Kohler (2019) in the context of nonparametric regression, up to a logarithm factor. Notably, the curse of dimensionality is mitigated here because  $d^*$  is strictly smaller than  $d$ .

Next, we establish a lower bound for the excess-risks of all classifiers from  $\mathcal{S}$  to  $\mathcal{H}$ . Recall that  $i^* \in \operatorname{argmin}_{i \in \{0, \dots, q\}} \tilde{\theta}_i / (2\tilde{\theta}_i + \tilde{k}_i)$ .

**Theorem 4.** *Suppose that the data  $\mathcal{D}$  is generated according to the distribution pair  $\mathcal{P}$ , and that the source data and target data in  $\mathcal{D}$  are independent of each other. Under the distribution class  $\mathcal{P}^*$  such that  $\tilde{k}_{i^*} \leq \min\{k_0, \dots, k_{i^*-1}\}$ , there exists a positive constant  $\zeta_7$  depending solely on  $(\tilde{\theta}_{i^*}, \tilde{k}_{i^*}, k)$  such that*

$$\inf_{\mathcal{A}: \mathcal{S} \rightarrow \mathcal{H}} \sup_{\mathcal{P} \in \mathcal{P}^*} \mathbb{E}_{\mathcal{D}} \{\mathcal{E}_Q(\mathcal{A}(\mathcal{D}))\} \geq \zeta_7 \left( \gamma_{n_P} + n_Q^{-1/2} \right). \quad (15)$$

The lower bound of the expected excess-risk, as established in Theorem 4, is contingent upon the condition  $\tilde{k}_{i^*} \leq \min\{k_0, \dots, k_{i^*-1}\}$ . This implies that no additional dimensions are incorporated at the intrinsic dimension level within the composite function, thereby precluding the scenario where  $\tilde{k}_{i^*}$  surpasses the covariate dimension  $d$ . Notably, the lower bound result in Theorem 4 retains its validity when the condition is fortified to  $\tilde{k}_i \leq \min\{k_0, \dots, k_{i-1}\}$  for all  $1 \leq i \leq k$  (See, e.g., Schmidt-Hieber (2020)). This signifies that no dimensions are added on deeper abstraction levels in the composition of functions.

According to Theorem 4, the convergence rates of the expected excess-risk for all classifiers transitioning from  $\mathcal{S}$  to  $\mathcal{H}$  do not surpass  $\gamma_{n_P} + n_Q^{-1/2}$ . In the meantime, Theorem 3 indicates that the convergence rate of the expected excess-risk for the proposed classifier  $\hat{f}$  is no slower than  $\gamma_{n_P} \log^2 n_P + n_Q^{-1/2}$ ; see inequality (14). Combining these results, we immediately deduce the minimax optimal rate for all classifiers and establish the minimax optimality of the proposed classifier  $\hat{f}$ .

**Corollary 1.** *Assume the conditions in Theorems 3 and 4. Then, the minimax optimal rate of convergence for all classifiers from  $\mathcal{S}$  to  $\mathcal{H}$  is  $\gamma_{n_P} + n_Q^{-1/2}$  up to a logarithm factor  $\log^2(n_P)$ , and the proposed classifier  $\hat{f}$  attains this optimal rate asymptotically.*

**Remark 1.** *In nonparametric binary classification problems, a commonly employed condition is the marginal assumption, which posits the existence of constants  $C_0 >$*

0 and  $\alpha \geq 0$  such that either  $Q(0 < |\eta_{Q,1}^0(X) - 0.5| \leq t) \leq C_0 t^\alpha$  (Audibert and Tsybakov, 2007; Maity et al., 2022) or  $Q(|\eta_{Q,1}^0(X) - 0.5| < t) \leq C_0 t^\alpha$  (Cai and Wei, 2021) holds for all  $t > 0$ . However, in our nonparametric classification setting, as outlined in Assumption (3), we refrain from employing such an assumption for two primary reasons. Firstly, the margin assumption can often be violated. For example, in binary classification scenarios, this assumption fails when  $\eta_{Q,1}^0(X)$  equals 0.5 with a positive probability. Secondly, verifying the margin assumption is challenging due to the unavailability of the target data labels. When the optimal rates derived in Maity et al. (2022, 2024) and Cai and Wei (2021) become more favorable as the parameter  $\alpha$  in the margin assumption increases (indicating a stronger margin assumption), the rates still depend on the covariate dimension  $d$ . Consequently, their methods remain susceptible to the curse of dimensionality.

In the context of binary classification, Maity et al. (2022) derived a lower bound for the expected excess-risk of all classifiers using labelled source data and unlabelled target data. Specifically, when the margin assumption is violated (i.e.,  $\alpha = 0$ ), the optimal rate obtained in Maity et al. (2022) [Theorem 12] is of the order  $n_P^{\frac{-\tilde{\beta}}{2\tilde{\beta}+d}} + n_Q^{-1/2}$ , where  $\tilde{\beta}$  represents the smoothness index of the probability density functions  $f_1(X)$  and  $f_2(X)$ . Notably, in scenarios where the intrinsic dimension of the composite function  $\phi_1^0$  is relatively low (as illustrated in Examples 1–2), the convergence rates presented in Theorems 3–4 surpass those of Maity et al. (2022) when  $d$  is large. When  $\phi_1^0$  is fully non-parametric, the convergence rate of our classifier aligns with that of Maity et al. (2022). However, under the margin assumption with  $\alpha > 0$  and when  $n_P = o(n_Q)$ , the optimal rate in Maity et al. (2022) is of the order  $n_P^{\frac{-\tilde{\beta}(1+\alpha)}{2\tilde{\beta}+d}}$ , which still suffers from the curse of dimensionality. In contrast, our classifier’s convergence rate is of the order  $\gamma_{n_P}$ , which is faster than that of Maity et al. (2022) when the intrinsic dimension of  $\phi_1^0$  is low and  $d$  is large.

## 5 Simulations

### 5.1 Methods under comparison

We conducted simulation experiments to assess the finite-sample performance of the proposed DNN and PMLE-based Classifier (DNN-PC) defined in (11). Although our DNN-PC is versatile and can be applied to multi-class classification problems, in this simulation study, we focused specifically on the binary-classification setting, where  $k = 2$ . The Bayes classifier for the target data is  $f(x) = 2 - I(\eta_{Q,1}(x) \geq 1/2)$ . For comparative purposes, we also include several popular competitors, which are variations of the Bayes classifier utilizing different estimates of  $\eta_{Q,1}(x)$ .

- Maity-PC: The classifier proposed by Maity *et al.* (2022), employs a PMLE. Specifically,  $\hat{P}_{X|Y=y}$  represents the kernel-density estimator of  $P_{X|Y=y}$  for  $y = 1, 2$ , and  $\tilde{\pi}_{Q,1}$  be the PMLE of  $\pi_{Q,1}$  obtained by replacing the estimates of  $P_{X|Y=1}/P_{X|Y=2}$  with the ratio of their kernel-density estimators. Maity-PC estimates  $\eta_{Q,1}(x)$  by

$$\tilde{\eta}_{Q,1}(x) = \frac{\tilde{\pi}_{Q,1}\hat{P}_{X|Y}(x | 1)}{\tilde{\pi}_{Q,1}\hat{P}_{X|Y}(x | 1) + (1 - \tilde{\pi}_{Q,1})\hat{P}_{X|Y}(x | 2)}.$$

- Saerens: This classifier, proposed by Saerens *et al.* (2002), estimates  $\eta_{P,1}$  using the K-nearest neighbors (KNN) method and  $\pi_{Q,1}$  using an Expectation-Maximization (EM) algorithm.
- Maity-IC: This is the ideal classifier proposed by Maity *et al.* (2022), which is essentially Maity-PC with  $\tilde{\pi}_{Q,1}$  replaced by the ideal estimator  $\hat{\pi}_{Q,\text{ideal}} = \sum_{j=1}^{n_Q} (2 - Y_j^Q)/n_Q$ .
- Maity-LA: This classifier, proposed by Maity *et al.* (2024), is based on a KNN estimator for  $\eta_{P,1}$  and Linear Adjustment model, which holds under GCS model.

The first three classifiers (DNN-PC, Maity-PC, and Saerens) are designed specifically for unsupervised transfer learning. The last two (Maity-IC and Maity-LA) are intended for supervised transfer learning, and are not applicable in our settings. However, they are included here solely for comparison purposes.

To implement the proposed DNN-PC method, we utilize the *Adam* optimizer in the *Deep Learning Toolbox* of Matlab to solve the optimization problem defined in (6).

Subsequently, we calculate the maximizer of the log-partial likelihood presented in (8) by resolving the associated score equation. This process is facilitated by the *fzero* solver available in Matlab.

The methods under comparison involves numerous hyperparameters. Specifically, in the proposed DNN-PC method, the hyperparameters include the number of hidden layer, the number of neurons per hidden layer, the learning rate, and mini-batch size utilized by the *Adam* optimizer (Kingma, 2014). Notably, we maintain a consistent number of neurons across all hidden layers in the pertinent DNN. The implementations of Maity-IC and Maity-PC involve kernel-based estimators, where we adopt the standard normal density function as the kernel function and consider the bandwidth as a hyperparameter. For the implementations of Maity-LA and Saerens, we regard the neighborhood size in K-NN as a hyperparameter. All these hyperparameters are selected through grid search.

## 5.2 Simulation settings

We generate  $Y^P$  and  $Y^Q$  such that  $2 - Y^P$  follows a Bernoulli distribution with success probability 0.75, and  $2 - Y^Q$  follows a Bernoulli distribution with success probability  $\pi_{Q,1}$ , where  $\pi_{Q,1}$  is considered to be either 0.25 (representing an imbalanced case) or 0.5 (representing a balanced case). The covariate  $X = (X_{(1)}, X_{(2)}, X_{(3)}, X_{(4)})^\top$  is chosen to be a 4-dimensional vector. Given  $Y = y$ , the components of  $X$ , denoted as  $X_{(i)}$ , are independent and identically distributed in both the source and target populations. Three scenarios are considered for the conditional distribution pairs. Given  $Y = y$ ,

- I. Both  $X_{(i)}^P$  and  $X_{(i)}^Q$  follow  $I(y = 1) \times \text{Uniform}(4) + I(y = 2) \times \text{Uniform}(2)$ , where  $\text{Uniform}(\tilde{\delta})$  denotes the discrete uniform distribution on  $\{1, \dots, \tilde{\delta}\}$  for  $\tilde{\delta} \in \mathbb{N}_+$ ;
- II. Both both  $X_{(i)}^P$  and  $X_{(i)}^Q$  follow  $I(y = 1) \times \text{Beta}(6, 2) + I(y = 2) \times \text{Beta}(2, 6)$ , where  $\text{Beta}(a, b)$  is the Beta distribution with shape parameters  $a > 0$  and  $b > 0$ ;
- III.  $X_{(i)}^P$  follow  $I(y = 1) \times \text{Exp}(e^{0.5} - 1) + I(y = 2) \times \text{Norm}(1, 1)$  and  $X_{(i)}^Q$  follow  $I(y = 1) \times \text{Exp}(1 - e^{-0.5}) + I(y = 2) \times \text{Norm}(0, 1)$ . Here,  $\text{Exp}(\mu_1)$  is the exponential distribution with mean  $\mu_1 > 0$  and  $\text{Norm}(\mu_2, \sigma)$  denotes the normal distribution with mean  $\mu_2 \in \mathbb{R}$  and standard deviation  $\sigma > 0$ .

The first two scenarios are specifically crafted to ensure that both the label shift and

GCS assumptions are met. In these scenarios, the conditional distributions of  $X_{(i)}$  given  $Y$  are discrete and continuous, respectively. However, in Scenario III, the label shift assumption is violated, while our GCS assumption remains valid with  $h(x) = \exp(2 + \beta^\top x)$ , where  $\beta = (-1, -1, -1, -1)^\top$ . Let  $p(t|y)$  represent the conditional probability density or mass function of  $X_{(i)}^P$  given  $Y^P = y$ . According to the aforementioned data generation settings, we have  $\eta_{P,1}(x) = \exp(\phi_1(x))/(1 + \exp(\phi_1(x)))$ , where  $\phi_1(x) = g_2 \circ g_1 \circ g_0(x)$  and  $g_2(t) = \log\{t/(1-t)\}$ ,  $g_1(a, b) = 3a/(3a+b)$  and  $g_0(x) = (\prod_{i=1}^4 p(x_{(i)} | 1), \prod_{i=1}^4 p(x_{(i)} | 2))$ .

When generating data, we set the sample size pairs  $(n_P, n_Q)$  to  $(100 \times J, 400)$  with  $J \in \{1, 2, 3, 5, 6\}$ . To approximate the excess-risk of a generic classifier, we utilize an independent test sample of size 2500 to compute its empirical excess-risk. The entire procedure is repeated 200 times, and the final reported excess-risk of the classifier is determined by averaging the 200 empirical excess-risks obtained.

### 5.3 Simulation results

Figure 5.3 presents the excess-risk results of the compared classifiers for different values of  $n_P$  and  $n_Q = 400$ . Scenarios I and II are crafted to meet the label shift assumption. In Scenario I, the covariates have discrete values and the  $\phi_1(\cdot)$  function is not a composite smoothness function, thus violating our Assumption 3. Nevertheless, the proposed DNN-PC classifier consistently exhibits less excess-risk compared to all four competing classifiers, even though Maity-IC and Maity-LA make the label information of the target data. A possible reason for this observation is that the kernel and KNN methods underlying the four competitors may have poor performance for discrete covariates.

In Scenario II, the proposed DNN-PC classifier remains uniformly superior to Saerens and Maity-LA, both of which are based on KNN. However, it shows comparable performance to Maity-PC and Maity-IC, which rely on the kernel method. This is likely due to the covariates being continuous in Scenario II, for which the kernel density estimator functions effectively. Additionally, the competing classifiers necessitate the estimation of  $P_{X|Y}(x|1), \dots, P_{X|Y}(x|k)$ , while our DNN-PC classifier only requires the estimation of their ratios, not the densities themselves. Generally, estimating the



conditional densities  $P_{X|Y}(x|i)$  is more difficult than estimating their ratios. Since the ideal classifier depends solely on the ratios, by directly estimating the ratios, our method not only reduces the number of parameters (the baseline conditional density or mass function) but also yields more reliable results than the competitors.

Scenario III is designed to violate the label shift assumption while satisfying the GCS assumption. Clearly, in terms of excess-risk, the proposed DNN-PC classifier uniformly outperforms the four competitors, regardless of whether the competitors incorporate the label information of the target data or not.

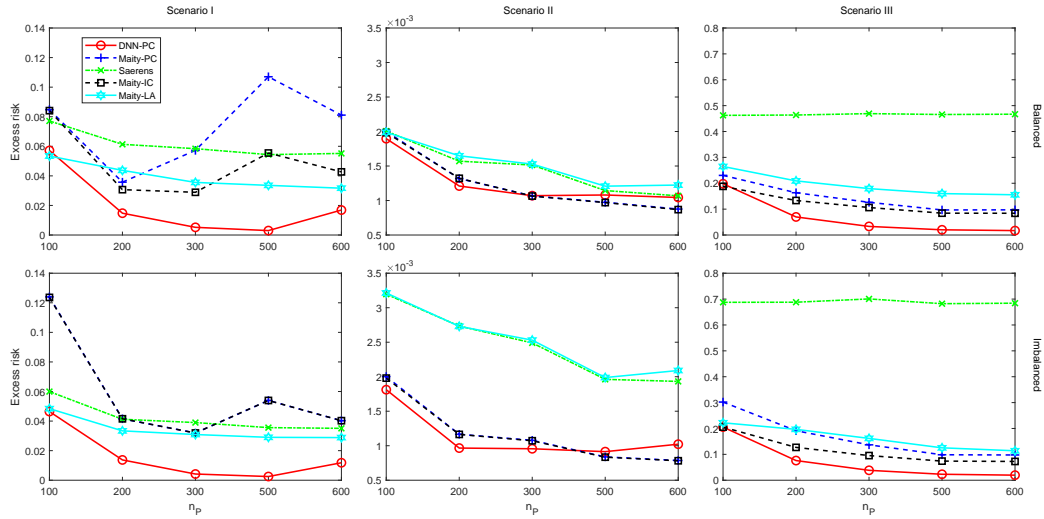


Figure 2: Plots of  $n_P$  versus excess-risks of the classifiers under comparison when  $n_Q = 400$ . Upper panel: the balanced case ( $\pi_{Q,1} = 0.5$ ); Lower panel: the unbalanced case ( $\pi_{Q,1} = 0.25$ )

The class proportions  $\pi_{Q,1}$  are crucial for the Bayes classifier in the target population. Among the classification methods being compared, three estimators for  $\pi_{Q,1}$  were utilized: (1) DNN: The proposed PMLE  $\hat{\pi}_{Q,1}$ , where the density ratio  $P_{X|Y=1}/P_{X|Y=2}$  is estimated using the proposed DNN estimators. (2) Kernel: The PMLE  $\tilde{\pi}_{Q,1}$  from Maity-PC, with the density ratio estimate replaced by the ratio of their kernel estimators, and (3) KNN: The estimator  $\hat{\pi}_{Q,EM}$  from Saerens *et al.* (2002), based on an EM algorithm after estimating  $\eta_{P,1}(\cdot)$  using K-NN estimators. Figure 5.3 displays the mean square error (MSE) results of these three estimators for  $\pi_{Q,1}$  when data were generated according to Scenarios I–III. In terms of MSE, the DNN estimator for  $\pi_{Q,1}$  is comparable to Kernel and KNN in Scenarios I and II, but

consistently outperforms the latter two in Scenario III. Notably, the superiority of our classifier often aligns with the superiority of our DNN estimator of  $\pi_{Q,1}$  compared to its competitors.

Additional simulations were conducted with sample size pairs  $(n_P, n_Q)$  set to  $(400, 100 \times J)$  for  $J \in \{1, 2, 3, 5, 6\}$  when data were generated according to Scenarios I-III. The corresponding results are presented in Section 7 of the supplementary material. Among the compared methods, our proposed classifier still exhibits the smallest excess-risk in Scenarios I and III. In Scenario II, its performance is comparable to the kernel-based classifiers (Maity-PC and Maity-IC), and they three uniformly outperform the KNN-based classifiers (Saerens and Maity-LA). Similarly, in estimating  $\pi_{Q,1}$ , our DNN estimator outperforms the kernel and KNN estimators in Scenarios I and III, and they are comparable in Scenario II. Unlike the case where  $n_P$  varies, the excess-risk and MSE remain relatively unchanged as  $n_Q$  increases from 100 to 600 with  $n_P$  fixed at 400.

Overall, the proposed estimation method and classifier are comparable or superior to existing competitors when the label shift assumption is satisfied and uniformly outperform them when the label shift assumption is violated but GCS is satisfied. Our method is capable of producing a more precise classifier, even with limited data availability in the target domain, while simultaneously demonstrating remarkable generalization ability and efficiency.

## 6 Diagnosis of Alzheimer’s Disease

Alzheimer’s disease represents a progressive neurological affliction that induces the degeneration and death of brain cells. This process leads to a consistent deterioration in cognitive faculties and functional capabilities. At present, approximately 50 million individuals globally are living with Alzheimer’s disease. Alarmingly, this figure is forecasted to double every five years, with projections indicating that it will surge to 152 million by the year 2050. The accurate diagnosis of Alzheimer’s disease holds paramount significance. It is crucial for effective disease treatment, providing support to patients and their families, and ensuring the proper allocation of medical resources.

In this section, we employ the proposed classification method to analyze the

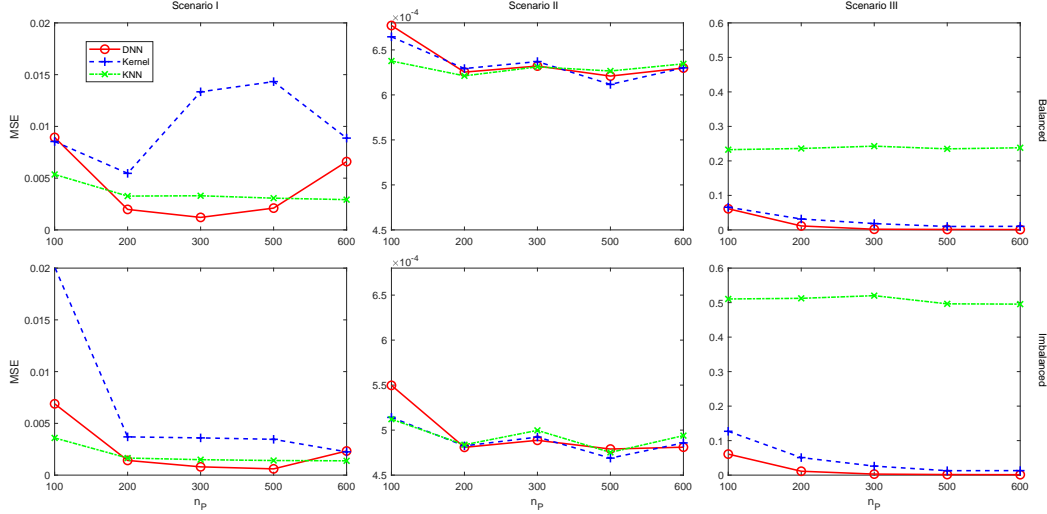


Figure 3: Mean square errors of the three estimators of  $\pi_{Q,1}$  under comparison with  $n_Q = 400$ . Upper panel: the balanced case ( $\pi_{Q,1} = 0.5$ ); Lower panel: the unbalanced case ( $\pi_{Q,1} = 0.25$ )

Alzheimer’s Disease Dataset of Kharoua (2024). This dataset encapsulates comprehensive health information for 2,149 patients, encompassing demographic specifics, lifestyle factors, medical histories, clinical measurements, cognitive and functional evaluations, symptoms, and Alzheimer’s disease diagnoses. We designate the Alzheimer’s disease diagnosis for each patient (with 1 indicating a positive diagnosis and 2 indicating a negative one) as the outcome variable  $Y$ , where  $k = 2$ . Our analysis includes 18 covariate variables, spanning demographic details (age and gender, comprising 2 variables), lifestyle factors (body mass index, alcohol consumption, physical activity, diet quality, and sleep quality, totaling 5 variables), medical history (family history of Alzheimer’s and cardiovascular disease, making up 2 variables), clinical measurements (systolic blood pressure, diastolic blood pressure, total cholesterol levels, low-density lipoprotein cholesterol levels, high-density lipoprotein cholesterol levels, and triglyceride levels, amounting to 6 variables), and cognitive and functional assessments (minimal state examination score, functional assessment score, and activities of daily living score, comprising 3 variables). The dataset, along with a detailed description of the covariates, is accessible via the URL <https://www.kaggle.com/datasets/rabieelkharoua/alzheimers-disease-dataset?resource=download>.

We categorize patients who smoke as belonging to the target domain ( $n_Q = 620$ )

and consider non-smoking patients as part of the source domain ( $n_P = 1529$ ). Our focus is on training a classification model that can predict whether a patient in the target domain has Alzheimer’s disease. Prior to our analysis, all covariates were scaled to fall within the range of 0 to 1. To assess the validity of the label shift assumption, we introduce an indicator variable  $D$ , assigning  $D = 1$  to all target data and  $D = 0$  to all source data. The label shift assumption translates to the conditional independence of the covariate vector  $X$  and the indicator  $D$ , given the outcome variable  $Y$ . We verify this conditional independence using the Invariant Conditional Quantile Prediction method (Heinze-Deml *et al.*, 2018), available within the R package `CondIndTests`. The resulting  $p$ -value of 0.0198 suggests insufficient evidence to uphold the label shift assumption.

When  $k = 2$ , the GCS assumption (2) is equivalent to  $r_1(x) - r_2(x) = 0$  for all  $x$ , where  $r_y(x) = Q_{X|Y}(x | y) / P_{X|Y}(x | y)$  for  $y = 1, 2$ . To verify the GCS assumption, we need to ensure that  $r_1(x) - r_2(x) = 0$  for all  $x$ . We randomly divide the dataset into two halves, designating one half for training and the other for testing. For each  $y = 1$  and 2, we combine the data  $X_Q$  and  $X_P$  with the same  $Y$  value and estimate the density ratio  $r_y(x)$  using a logistic regression model (Qin, 1998). Figure 6 presents histograms depicting the estimated density ratios  $r_1(x)$  and  $r_2(x)$ , as well as their difference  $r_1(x) - r_2(x)$ , evaluated at the covariates of the test data. It is evident from Figure 6(a) that the histograms of  $r_1(x)$  and  $r_2(x)$  are highly similar. Furthermore, Figure 6(b) reveals that most of their difference values are close to zero. Both observations lend support to our GCS assumption.

We apply the proposed estimation and classification method and its competitors presented in Section 5 to predict the diagnosis results of the patients in the target domain. The samples in the target domain are randomly partitioned into training and validation sets, with the training set consisting of  $100p\%$  of the total target data, where  $p = 0.5, 0.6, \text{ or } 0.7$ . Although the target data here are all labeled, we consider the labels of the training set of the target data as missing when applying DNN-PC, Maity-PC, and Saerens. The correct classification proportion of each classifier is evaluated based on the validation data. The left plot of Figure 6 shows the proportions of correct classification or correct diagnosis of the five classifiers under comparison for the three choices of  $p$ . It is evident that our DNN-PC consistently has the largest

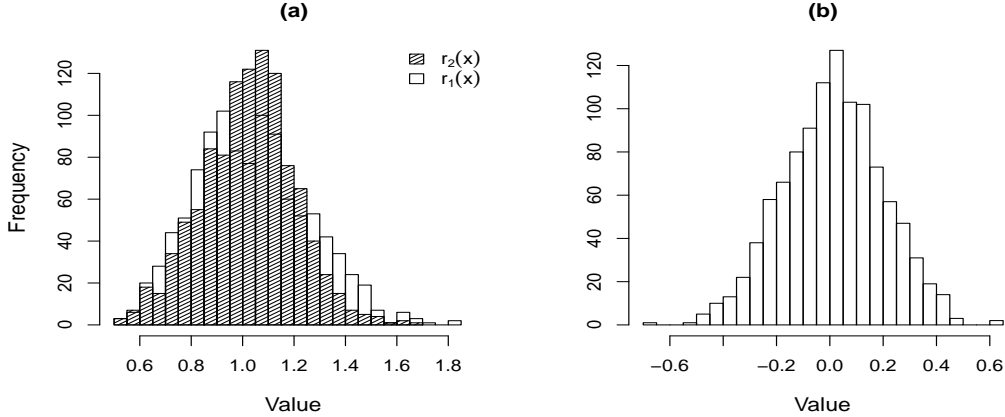


Figure 4: Histograms of estimated density ratios  $r_1(x)$  and  $r_2(x)$  (plot (a)), and their difference  $r_1(x) - r_2(x)$  (plot (b)) evaluated at the covariates of the test data.

correct classification proportion among all five classifiers, indicating that our classifier yields the most accurate diagnosis results. The right plot of Figure 6 presents the absolute relative biases of the three estimators (DNN, Kernel, and KNN) of  $\pi_{Q,1}$  when we take the proportion of label 1 in the target data as the true value of  $\pi_{Q,1}$ . The plot reveals that the absolute relative bias of our DNN-based PMLE (i.e., DNN) is significantly smaller than those of the Kernel and KNN estimates. In particular, for different choices of  $p$ , the absolute relative biases of DNN are no greater than 10%, whereas those of both Kernel and KNN are no less than 15%. These results once again affirm the superiority of the proposed classifier and proportion estimation method over the existing competitors.

## 7 Discussion

Deep learning and transfer learning have exhibited their potential across numerous domains. Under a novel GCS assumption, this paper explores the domain of deep transfer learning within the framework of classification that is based on a group of labelled source data and unlabelled target data. We meticulously establish concentration bounds for the proposed DNN estimator of the classification function and the PMLE of the class proportion of the target domain. We construct a Bayes classifier for the target domain using these two estimators and prove that it is minimax

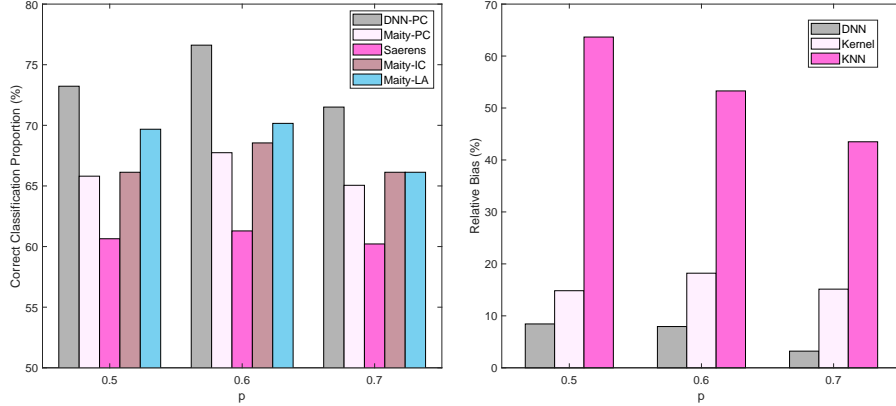


Figure 5: Plots of analysis results for the Alzheimer’s Disease Dataset when  $p = 0.5, 0.6,$  or  $0.7$ . Left plot: Correct classification proportions of the five classifiers under comparison. Right plot: Absolute relative bias of DNN, Kernel and KNN with respect to the proportion of label 1 in the target data.

optimal in terms of excess-risk. Thanks to the remarkable approximation capability of DNN, the proposed classifier can circumvent the notorious curse-of-dimensionality issue and showcases impressive numerical performance regarding both accuracy and efficiency.

In our analysis of the Alzheimer’s Disease dataset, a histogram-based visual comparison method is employed to justify the GCS assumption; however, it lacks the rigor of quantitative analysis. This thereby raises the question of how to construct a valid hypothesis test for checking the GCS assumption based on labelled source data and unlabelled target data. Intuitively, a test statistic can be constructed by measuring the deviation from GCS. For instance, we might use the overall absolute difference between  $\hat{r}_1(x), \dots, \hat{r}_k(x)$ , where  $r_y(x) = Q_{X|Y}(x | y) / P_{X|Y}(x | y)$  and  $\hat{r}_y(x)$  is its estimate. Nevertheless, it is quite challenging to derive the limiting distribution of this measure under the GCS assumption. We may leave this issue for future research.

## Supplementary information

The supplementary material contains proofs of all the theorems and lemmas, and provides additional simulation results.

# Acknowledgements

Liu’s research is supported by the National Natural Science Foundation of China (12371293, 12171157, 32030063), Fundamental Research Funds for the Central Universities and the 111 Project (B14019).

# References

- Alexandari, A., Kundaje, A., and Shrikumar, A. (2020). Em with bias-corrected calibration is hard-to-beat at label shift adaptation. In *Proceedings of the 37th International Conference on Machine Learning, Vienna, Austria, PMLR 119*. PMLR.
- Audibert, J.-Y. and Tsybakov, A. B. (2007). Fast learning rates for plug-in classifiers. *The Annals of Statistics*, **35**(2), 608–633.
- Azizzadenesheli, K., Liu, A., Yang, F., and Anandkumar, A. (2019). Regularized learning for domain adaptation under label shifts. *arXiv preprint arXiv:1903.09734*.
- Bauer, B. and Kohler, M. (2019). On deep learning as a remedy for the curse of dimensionality in nonparametric regression. *The Annals of Statistics*, **47**(4), 2261–2285.
- Ben-David, S., Lu, T., Luu, T., and Pal, D. (2010). Impossibility theorems for domain adaptation. In *International Conference on Artificial Intelligence and Statistics (AISTATS), 2010*.
- Cai, T. T. and Wei, H. (2021). Transfer learning for nonparametric classification: Minimax rate and adaptive classifier. *The Annals of Statistics*, **49**(1), 100–128.
- Chen, X., Liu, Y., Ma, S., and Zhang, Z. (2024). Causal inference of general treatment effects using neural networks with a diverging number of confounders. *Journal of Econometrics*, **238**(1), 105555.
- Chernozhukov, V., Chetverikov, D., Demirer, M., Duflo, E., Hansen, C., Newey, W., and Robins, J. (2018). Double/debiased machine learning for treatment and structural parameters. *The Econometrics Journal*, **21**(1), C1–C68.

- Dempster, A., Laird, N., and Rubin, D. (1977). Maximum likelihood from incomplete data via the em algorithm (with discussion). *Journal of the Royal Statistical Society, Series B*, **39**, 1–38.
- Garg, S., Wu, Y., Balakrishnan, S., and Lipton, Z. (2020). A unified view of label shift estimation. *Advances in Neural Information Processing Systems*, **33**, 3290–3300.
- Glorot, X., Bordes, A., and Bengio, Y. (2011). Deep sparse rectifier neural networks. *Aistats. Proceedings of Machine Learning Research*, **15**, 315–323.
- Han, S., Pool, J., Tran, J., and Dally, W. (2015). Learning both weights and connections for efficient neural network. *Advances in neural information processing systems*, **28**, 1135–1143.
- Heinze-Deml, C., Peters, J., and Meinshausen, N. (2018). Invariant causal prediction for nonlinear models. *Journal of Causal Inference*, **6**(2), 20170016.
- Horowitz, J. L. and Mammen, E. (2007). Rate-optimal estimation for a general class of nonparametric regression models with unknown link functions. *The Annals of Statistics*, **35**(6), 2589 – 2619.
- Huang, J.-T., Li, J., Yu, D., Deng, L., and Gong, Y. (2013). Cross-language knowledge transfer using multilingual deep neural network with shared hidden layers. In *2013 IEEE international conference on acoustics, speech and signal processing*, pages 7304–7308. IEEE.
- Ichimura, H. (1993). Semiparametric least squares (sls) and weighted sls estimation of single-index models. *Journal of Econometrics*, **59**, 71–120.
- Imaizumi, M. and Fukumizu, K. (2019). Deep neural networks learn non-smooth functions effectively. In *The 22nd international conference on artificial intelligence and statistics*, pages 869–878. PMLR.
- Iman, M., Arabnia, H. R., and Rasheed, K. (2023). A review of deep transfer learning and recent advancements. *Technologies*, **11**(2), 40.



- Iyer, A., Nath, S., and Sarawagi, S. (2014). Maximum mean discrepancy for class ratio estimation: Convergence bounds and kernel selection. In *International conference on machine learning*, pages 530–538. PMLR.
- Jain, S., White, M., and Radivojac, P. (2016). Estimating the class prior and posterior from noisy positives and unlabeled data. *Advances in neural information processing systems*, **29**.
- Jiao, Y., Shen, G., Lin, Y., and Huang, J. (2023). Deep nonparametric regression on approximate manifolds: Nonasymptotic error bounds with polynomial prefactors. *The Annals of Statistics*, **51**(2), 691–716.
- Kharoua, R. E. (2024). Alzheimer’s disease dataset.
- Kingma, D. (2014). Adam: a method for stochastic optimization. *arXiv preprint arXiv:1412.6980*.
- Kohler, M. and Krzyżak, A. (2016). Nonparametric regression based on hierarchical interaction models. *IEEE Transactions on Information Theory*, **63**(3), 1620–1630.
- Kpotufe, S. and Martinet, G. (2021). Marginal singularity and the benefits of labels in covariate-shift. *The Annals of Statistics*, **49**, 3299–3323.
- Lee, S. h., Ma, Y., and Zhao, J. (2024). Doubly flexible estimation under label shift. *Journal of the American Statistical Association*, pages 1–13.
- Lipton, Z., Wang, Y.-X., and Smola, A. (2018). Detecting and correcting for label shift with black box predictors. In *International conference on machine learning*, pages 3122–3130. PMLR.
- Liu, R., Li, K., and Shang, Z. (2020). A computationally efficient classification algorithm in posterior drift model: phase transition and minimax adaptivity. *arXiv preprint arXiv:2011.04147*.
- Liu, X., Guo, Z., Li, S., Xing, F., You, J., Kuo, C.-C. J., El Fakhri, G., and Woo, J. (2021). Adversarial unsupervised domain adaptation with conditional and label shift: Infer, align and iterate. In *Proceedings of the IEEE/CVF international conference on computer vision*, pages 10367–10376.

- Ma, S. and He, X. (2016). Inference for single-index quantile regression models with profile optimization. *The Annals of Statistics*, **44**(3), 1234 – 1268.
- Maity, S., Sun, Y., and Banerjee, M. (2022). Minimax optimal approaches to the label shift problem in non-parametric settings. *Journal of Machine Learning Research*, **23**(346), 1–45.
- Maity, S., Yurochkin, M., Banerjee, M., and Sun, Y. (2023). Understanding new tasks through the lens of training data via exponential tilting. In *The Eleventh International Conference on Learning Representations*.
- Maity, S., Dutta, D., Terhorst, J., Sun, Y., and Banerjee, M. (2024). A linear adjustment-based approach to posterior drift in transfer learning. *Biometrika*, **111**(1), 31–50.
- Miao, K. H. and Miao, J. H. (2018). Coronary heart disease diagnosis using deep neural networks. *International Journal of Advanced Computer Science and Applications*, **9**(10).
- Pedamonti, D. (2018). Comparison of non-linear activation functions for deep neural networks on mnist classification task. *Preprint, arXiv:1804.02763*.
- Qin, J. (1998). Inferences for case-control and semiparametric two-sample density ratio models. *Biometrika*, **85**(3), 619–630.
- Reeve, H. W., Cannings, T. I., and Samworth, R. J. (2021). Adaptive transfer learning. *The Annals of Statistics*, **49**(6), 3618–3649.
- Robins, J. M., Rotnitzky, A., and Zhao, L. P. (1994). Estimation of regression coefficients when some regressors are not always observed. *Journal of the American statistical Association*, **89**(427), 846–866.
- Saerens, M., Latinne, P., and Decaestecker, C. (2002). Adjusting the outputs of a classifier to new a priori probabilities: a simple procedure. *Neural computation*, **14**, 21–41.

- Sarikaya, R., Hinton, G. E., and Deoras, A. (2014). Application of deep belief networks for natural language understanding. *IEEE/ACM Transactions on Audio, Speech, and Language Processing*, **22**(4), 778–784.
- Schmidt-Hieber, J. (2020). Nonparametric regression using deep neural networks with ReLU activation function. *The Annals of Statistics*, **48**(4), 1875–1897.
- Shen, G., Jiao, Y., Lin, Y., Horowitz, J. L., and Huang, J. (2024). Nonparametric estimation of non-crossing quantile regression process with deep requ neural networks. *Journal of Machine Learning Research*, **25**(88), 1–75.
- Srinivas, S., Subramanya, A., and Venkatesh Babu, R. (2017). Training sparse neural networks. In *Proceedings of the IEEE conference on computer vision and pattern recognition workshops*, pages 138–145.
- Stone, C. J. (1982). Optimal global rates of convergence for nonparametric regression. *The Annals of Statistics*, **10**, 1040–1053.
- Stone, C. J. (1985). Additive regression and other nonparametric models. *The Annals of Statistics*, **13**(2), 689–705.
- Sugiyama, M., Nakajima, S., Kashima, H., Buenau, P. V., and Kawanabe, M. (2008). Classifying titanic passenger data and prediction of survival from disaster. In *Advances in Neural Information Processing Systems*, page 1433i<sub>2</sub>C1440.
- Szegedy, C., Liu, W., Jia, Y., Sermanet, P., Reed, S., Anguelov, D., Erhan, D., Vanhoucke, V., and Rabinovich, A. (2015). Going deeper with convolutions. In *Proceedings of the IEEE conference on computer vision and pattern recognition*, pages 1–9.
- Tan, C., Sun, F., Kong, T., Zhang, W., Yang, C., and Liu, C. (2018). A survey on deep transfer learning. In *Artificial Neural Networks and Machine Learning–ICANN 2018: 27th International Conference on Artificial Neural Networks, Rhodes, Greece, October 4-7, 2018, Proceedings, Part III 27*, pages 270–279. Springer.

- Tzeng, E., Hoffman, J., Saenko, K., and Darrell, T. (2017). Adversarial discriminative domain adaptation. In *Proceedings of the IEEE conference on computer vision and pattern recognition*, pages 7167–7176.
- Weiss, K., Khoshgoftaar, T. M., and Wang, D. (2016). A survey of transfer learning. *Journal of Big data*, **3**, 1–40.
- Yarotsky, D. (2017). Error bounds for approximations with deep relu networks. *Neural Networks*, **94**, 103–114.
- Zhang, K., Schölkopf, B., Muandet, K., and Wang, Z. (2013). Domain adaptation under target and conditional shift. In *International conference on machine learning*, pages 819–827. Pmlr.
- Zhong, Q., Mueller, J., and Wang, J.-L. (2022). Deep learning for the partially linear Cox model. *The Annals of Statistics*, **50**(3), 1348–1375.
- Zhuang, F., Qi, Z., Duan, K., Xi, D., Zhu, Y., Zhu, H., Xiong, H., and He, Q. (2020). A comprehensive survey on transfer learning. *Proceedings of the IEEE*, **109**(1), 43–76.